J Biol Inorg Chem (2009) 14:485–496
DOI 10.1007/s00775-008-0464-6

ORIGINAL PAPER

Effects of selenium on the structure and function of recombinant human *S*-adenosyl-L-methionine dependent arsenic (+3 oxidation state) methyltransferase in *E. coli*

Zhirong Geng · Xiaoli Song · Zhi Xing · Jinlong Geng · Sichun Zhang · Xinrong Zhang · Zhilin Wang

Received: 17 August 2008 / Accepted: 26 December 2008 / Published online: 22 January 2009

Abstract The effects of Se^{IV} on the structure and function of recombinant human arsenic (+3 oxidation state) methyltransferase (AS3MT) purified from the cytoplasm of *Escherichia coli* were studied. The coding region of human AS3MT complementary DNA was amplified from total RNA extracted from HepG2 cell by reverse transcription PCR. Soluble and active human AS3MT was expressed in the *E. coli* with a Trx fusion tag under a lower induction temperature of 25 °C. Spectra (UV–vis, circular dichroism, and fluorescence) were first used to probe the interaction of Se^{IV} and recombinant human AS3MT and the structure–function relationship of the enzyme. The recombinant human AS3MT had a secondary structure of 29.0% α-helix, 23.9% β-pleated sheet, 17.9% β-turn, and 29.2% random coil. When Se^{IV} was added, the content of the α-helix did not change, but that of the β-pleated sheet increased remarkably in the conformation of recombinant human AS3MT. Se^{IV} inhibited the enzymatic methylation of inorganic As^{III} in a concentration-dependent manner. The IC_{50} value for Se^{IV} was 2.38 μM. Double-reciprocal ($1/V$ vs. $1/[\text{inorganic } As^{III}]$) plots showed Se^{IV} to be a noncompetitive inhibitor of the methylation of inorganic As^{III} by recombinant human AS3MT with a K_i value of 2.61 μM. We hypothesized that Se^{IV} interacts with the sulfhydryl group of cysteine(s) in the structural residues rather than the cysteines of the active site (Cys156 and Cys206). When Se^{IV} was combined with cysteine(s) in the structural residues, the conformation of recombinant human AS3MT changed and the enzymatic activity decreased. Considering the quenching of tryptophan fluorescence, Cys72 and/or Cys226 are deduced to be primary targets for Se^{IV}.

Keywords Recombinant human arsenic (+3 oxidation state) methyltransferase · Circular dichroism spectrum · Selenium · Structure–function relationship · Noncompetitive inhibitor

Abbreviations

AS3MT	Arsenic (+3 oxidation state) methyltransferase
CD	Circular dichroism
cDNA	Complementary DNA
DMA^V	Dimethylarsinic acid
DTT	1,4-Dithiothreitol
GSH	Glutathione
iAs^{III}	Inorganic arsenite
iAs^V	Inorganic arsenate
IPTG	Isopropyl β-D-thiogalactopyranoside
MALDI	Matrix-assisted laser desorption/ionization

Z. Geng · X. Song · Z. Wang (✉)
State Key Laboratory of Coordination Chemistry,
School of Chemistry and Chemical Engineering,
Nanjing University,
Nanjing 210093,
People's Republic of China
e-mail: wangzl@nju.edu.cn

Z. Geng
e-mail: njugeng@gmail.com

Z. Xing · S. Zhang · X. Zhang
Key Laboratory for Atomic and Molecular Nanosciences
of Education Ministry,
Department of Chemistry,
Tsinghua University, Beijing 100084,
People's Republic of China

J. Geng
School of Science,
Nanjing Agricultural University,
Nanjing 210095,
People's Republic of China

2-ME	2-Mercaptoethanol
MMA^V	Monomethylarsonic acid
MS	Mass spectrometry
Ni-NTA	Nickel nitrilotriacetic acid
SAM	*S*-Adenosyl-L-methionine
SDS-PAGE	Sodium dodecyl sulfate polyacrylamide gel electrophoresis
Se^{IV}	Selenite
TOF	Time of flight
Tris–HCl	Tris(hydroxymethyl)aminomethane hydrochloride

Introduction

Inorganic arsenite (iAs^{III}) and inorganic arsenate (iAs^V) are important worldwide environmental toxicants of both natural and anthropogenic sources [1–4]. Chronic exposure to arsenic through contamination of drinking water can cause cardiovascular disease, neurologic and neurobehavioral disorders, and cancers of the skin, liver, lungs, bladder, and kidneys [5–8]. Methylation has been commonly regarded as the primary mechanism of detoxification of inorganic arsenic in mammals [9]. It is generally accepted that inorganic arsenicals are metabolized by arsenic (+3 oxidation state) methyltransferase (AS3MT), through repetitive reduction and oxidative methylation to form pentavalent methylated arsenicals, such as monomethylarsonic acid (MMA^V) and dimethylarsinic acid (DMA^V), which are excreted mainly in urine [10–16]. However, Hayakawa et al. [17] put forward a new putative enzymatic mechanism of methylation of inorganic arsenicals by human AS3MT. As a result, a new metabolic pathway of inorganic arsenic via an arsenic–glutathione (GSH) complex was developed. Thus, the mechanism of methylation, especially the factors affecting the methylation of iAs^{III}, such as selenium, should be studied further.

Selenium and arsenic are metalloids with similar chemical properties and metabolic conversions in vivo [18]. Inorganic selenium is first reduced by GSH to form selenodiglutathione, which is catalyzed to selenopersulfide and hydrogen selenide (H_2Se) by GSH reductase [19–21]. H_2Se, the putative intermediary metabolite, is enzymatically methylated by methyltransferase to methylselenol, CH_3SeH, dimethylselenide, $(CH_3)_2Se$, and trimethylselenonium cation, $(CH_3)_3Se^+$ [22–24]. Moreover, selenium and arsenic act as metabolic antagonists. For example, inorganic arsenic could antagonize the toxicity of inorganic selenium [25]. The effects of selenium on the metabolism of inorganic arsenic in organisms and cells, and even by rat liver cytosol and a recombinant rat AS3MT were studied [18, 26–36]. Selenite (Se^{IV}) was found to inhibit AS3MT activity, yet the mechanisms were unclear. The mechanisms perhaps include the interaction between arsenic and selenium and the direct interaction between selenium and AS3MT [28]. The formation of selenobis(*S*-glutathionyl)arsinium ion provided a molecular basis for the antagonistic interaction between arsenic and selenium [37–39]. The inhibition of enzyme activity by selenium compounds was attributed to their affinity for thiols at the active site of the enzyme [40]. Analysis of matrix-assisted laser desorption/ionization (MALDI) time of flight (TOF) mass spectra of hGSTO1-1 after reaction with GSH and Se^{IV} indicated that Se^{IV} was integrated into hGSTO1-1 molecules between the disulfides of GSH and the cysteines of hGSTO1-1 [40]. However, the interaction between selenium and recombinant human AS3MT had been seldom studied. The site(s) where selenium binds to the cysteine(s) of recombinant human AS3MT should also be studied further. In the structure model of mouse AS3MT raised by Fomenko et al. [41], active-site cysteine was surface-exposed and protein topology supported the formation of an intramolecular disulfide during the catalytic cycle. It is well known that human AS3MT has high homology with mouse AS3MT [15]. However the secondary structure of human AS3MT, especially the effect of selenium on the change of secondary structure of human AS3MT, had not been reported.

In this study, we describe several significant achievements in the *Escherichia coli* expression of human AS3MT and examine the effect of Se^{IV} on the methylation of iAs^{III}. Spectra (UV–vis, circular dichroism, CD, and fluorescence) were first utilized to probe the interaction of Se^{IV} and recombinant human AS3MT and the structure–function relationship of the enzyme. Se^{IV} was the potent inhibitor of iAs^{III} methylation by recombinant human AS3MT in a noncompetitive manner. The effects of Se^{IV} on the structure and activity were both concentration-dependent. The modification of the conformation of recombinant human AS3MT by Se^{IV} probably involved interactions with one or several cysteines in the structural residues of recombinant human AS3MT, not in the active site of the enzyme. Combined with the quenching of tryptophan fluorescence, Cys72 and/or Cys226 may be primary targets for Se^{IV}. Further study will be done on the site(s) where selenium binds to the cysteine(s) of human AS3MT by the use of site-directed mutagenesis.

Materials and methods

Caution: Inorganic arsenic [42] and sodium selenite have been classified as human carcinogens and should be handled accordingly.

Reverse transcription PCR

AS3MT has been reported to be expressed in the HepG2 human hepatoma cell line [14]. Total RNA was extracted from the cells using Trizol reagent at 0 °C. After the addition of chloroform, extracts were vortexed, incubated at room temperature, and centrifuged at 12,000*g* at 4 °C. RNA in the aqueous phase was precipitated with 2-propanol and pelleted by centrifugation at 4 °C. RNA pellets were washed with 75% ethanol and air dried for 10–20 min. With use of an RNA PCR kit (Takara) according to the manufacturer's instructions (forward primer 5′-ATGGCTGCACTTCGTGACGC-3′, reverse primer 5′-GATTTAGCAGCTTTTCTTTG-3′), the coding region of human AS3MT complementary DNA (cDNA) was amplified by reverse transcription PCR (Fig. 1). The PCR conditions were denaturation (30 s at 94 °C), annealing (30 s at 60 °C), and extension (1.5 min at 72 °C) for 30 cycles, and final extension (7 min at 72 °C) for one cycle.

Site-directed mutagenesis

There was a stable hairpin in the human *AS3MT* gene which was analyzed by RNAstructure 4.3 (Fig. 2). To eliminate the effect of the hairpin in the protein expression, the gene was modified using five synonymous codons according to the code bias of *E. coli*. Briefly, this step used the "megaprimer" method of site-directed mutagenesis by the use of three oligonucleotide primers and two rounds of PCR with PrimeSTAR HS DNA polymerase (Takara). One of the oligonucleotides is mutagenic (mutagenic primer 5′-CGG CCTcGCgGTGGTcACgCAaCCGTTG-3′); the other two are forward and reverse primers that lie upstream and downstream of the binding site for the mutagenic oligonucleotide (forward primer 5′-*GGATCC*ATGGCTGCACTT CGTGAC-3′, reverse primer: 5′-*GTCGAC*TTAGTGGTG GTGGTGGTGGTGGCAGCTTTTCTTTGT-3′). The forward primer contains a *Bam*HI restriction site, and the reverse primer has a sequence to encode the 6×His-tag and a *Sal*I site at the 3′ end immediately before and after the stop codon, respectively, to facilitate the cloning of the amplified product into the expression vector, pET-32a(+). The mutagenic primer and the forward primer were used in the first PCR to amplify a mutated fragment of the human *AS3MT* gene. The first PCR product, a 120-bp DNA fragment, was purified by an agarose gel DNA purification kit and was used as the megaprimer in the second PCR in conjunction with the reverse primer to amplify the full-length mutant gene of the template DNA. The modified human *AS3MT* gene was sequenced using the double-stranded dideoxy method

```
atggctgcacttcgtgacgctgagatacagaaggacgtgcagacctactacgggcaggtg
 M  A  A  L  R  D  A  E  I  Q  K  D  V  Q  T  Y  Y  G  Q  V
ctgaagagatcggcagacctccagaccaacggctgtgtcaccacagccaggccggtcccc
 L  K  R  S  A  D  L  Q  T  N  G  C  V  T  T  A  R  P  V  P
aagcacatccgggaagccttgcaaaatgtacacgaagaagtagccctaagatattatggc
 K  H  I  R  E  A  L  Q  N  V  H  E  E  V  A  L  R  Y  Y  G
tgtggtctggtgatccctgagcatctagaaaactgctggattttggatctgggtagtgga
 C  G  L  V  I  P  E  H  L  E  N  C  W  I  L  D  L  G  S  G
agtggcagagattgctatgtacttagccagctggttggtgaaaaaggacacgtgactgga
 S  G  R  D  C  Y  V  L  S  Q  L  V  G  E  K  G  H  V  T  G
atagacatgaccaaaggccaggtggaagtggctgaaaagtatcttgactatcacatggaa
 I  D  M  T  K  G  Q  V  E  V  A  E  K  Y  L  D  Y  H  M  E
aaatatggcttccaggcatctaatgtgacttttattcatggctacattgagaagttggga
 K  Y  G  F  Q  A  S  N  V  T  F  I  H  G  Y  I  E  K  L  G
gaggctggaatcaagaatgagagccatgatattgttgtatcaaactgtgttattaacctt
 E  A  G  I  K  N  E  S  H  D  I  V  V  S  N  C  V  I  N  L
gtgcctgataaacaacaagtgcttcaggaggcatatcgggtgctgaagcatggtggggag
 V  P  D  K  Q  Q  V  L  Q  E  A  Y  R  V  L  K  H  G  G  E
ttatatttcagtgacgtctatacgagccttgaactgccagaagaaatcaggacacacaaa
 L  Y  F  S  D  V  Y  T  S  L  E  L  P  E  E  I  R  T  H  K
gttttatggggtgagtgtctgggtggtgctttatactggaaggaacttgctgtccttgct
 V  L  W  G  E  C  L  G  G  A  L  Y  W  K  E  L  A  V  L  A
caaaaaattgggttctgccctccacgtttggtcactgccaatctcattacaattcaaaac
 Q  K  I  G  F  C  P  P  R  L  V  T  A  N  L  I  T  I  Q  N
aaggaactggaaagagttatcggtgactgtcgttttgtttctgcaacatttcgcctcttc
 K  E  L  E  R  V  I  G  D  C  R  F  V  S  A  T  F  R  L  F
aaacactctaagacaggaccaaccaagagatgccaagttatttacaatggaggaattaca
 K  H  S  K  T  G  P  T  K  R  C  Q  V  I  Y  N  G  G  I  T
ggacatgaaaaagaactaatgtttgatgccaattttacatttaaggaaggtgaaattgtt
 G  H  E  K  E  L  M  F  D  A  N  F  T  F  K  E  G  E  I  V
gaagtggatgaagaaacagcagctatcttgaagaattcaagatttgctcaagattttctg
 E  V  D  E  E  T  A  A  I  L  K  N  S  R  F  A  Q  D  F  L
atcagaccaattggagagaagttgccaacatctggaggctgttctgctttggagttaaag
 I  R  P  I  G  E  K  L  P  T  S  G  G  C  S  A  L  E  L  K
gatataatcacagatccatttaagcttgcagaagagtctgacagtatgaagtccagatgt
 D  I  I  T  D  P  F  K  L  A  E  E  S  D  S  M  K  S  R  C
gtccctgatgctgctggaggctgctgtggcacaaagaaaagctgctaaatc
 V  P  D  A  A  G  G  C  C  G  T  K  K  S  C  -
```

Fig. 1 Human arsenic (+3 oxidation state) methyltransferase (AS3MT) complementary DNA nucleotide and encoded amino acid sequences

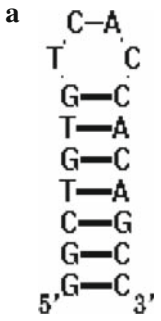

b WT: 5′GGC TGT GTC ACC ACA GCC3′

MU: 5′GG***T*** TG***C*** GT***G*** ACC AC***C*** GC***G***3′

AA: G C V T T A

Fig. 2 Hairpin of the human *AS3MT* gene and its modification. **a** Hairpin of the gene. **b** Hairpin sequence (*WT*), modification gene sequence (*MU*), and their common encoding amino acid sequence (*AA*). The *italics* indicate mutant sites

(described by Sanger et al. [43]) to ensure that no new sequence error was introduced during PCR amplification.

Protein expression and purification

The modified human *AS3MT* gene was inserted between the *Bam*HI and *Sal*I sites of the pET-32a vector to produce the expression plasmid pET-32a-*AS3MT*. Expression host, *E. coli* BL21 (DE3) pLysS (Novagen), was transformed by the ligated plasmid by heat shock (42 °C, 30 s) and the colonies were selected on standard ampicillin-containing agar plates and confirmed by restriction enzyme analysis. To express human AS3MT, *E. coli* was cultured to the mid-log phase (optical density at 600 nm 0.6–1.0) in 200 ml of Luria–Bertani broth medium (10 g tryptone, 5 g yeast extract, 10 g NaCl per liter) containing 100 μg/ml of ampicillin and then induced with 1 mM isopropyl-β-D-thiogalactopyranoside (IPTG) at 25 °C for 5 h. The cultured cells were centrifuged at 10,000*g* for 10 min at 4 °C, resuspended in 8 ml of ice-cold 1× binding buffer [20 mM tris(hydroxymethyl)aminomethane hydrochloride (Tris–HCl) buffer at pH 7.9 containing 0.5 M NaCl and 5 mM imidazole], sonicated on ice, and centrifuged at 14,000*g* for 20 min. The postcentrifugation supernatant was filtered through a 0.45-μm membrane to prevent clogging of resins, and loaded onto a 2.5 ml nickel nitrilotriacetic acid (Ni-NTA) agarose column (Novagen) at a flow rate of about 20 ml/h. The Ni-NTA agarose column was pre-equilibrated with three column volumes of 1× binding buffer. After adsorption of recombinant human AS3MT, the column was washed with ten column volumes of 1× binding buffer. Then the contamination proteins were eluted with six column volumes of 1× wash buffer (20 mM Tris–HCl buffer at pH 7.9 containing 0.5 M NaCl and 60 mM imidazole), and the recombinant protein (recombinant human AS3MT) was eluted with six column volumes of 1× elution buffer (20 mM Tris–HCl buffer at pH 7.9 containing 0.5 M NaCl and 1 M imidazole). The recombinant human AS3MT was dialyzed twice against sodium phosphate buffer to remove imidazole. The purified recombinant human AS3MT yielded a single band on sodium dodecyl sulfate polyacrylamide gel electrophoresis (SDS-PAGE). Protein concentration was measured by a Bradford assay based on a bovine serum albumin standard curve.

Analysis of recombinant human AS3MT by MALDI-TOF mass spectrometry

Removal of buffers and salts from protein samples was accomplished in accordance with the user guide of ZipTipC4 (Millipore). The tip was prewetted twice with wetting buffer (50% acetonitrile in water), and equilibrated twice with equilibration buffer (0.1% trifluoroacetic acid in water). The recombinant human AS3MT samples could then be applied and the flow-through fraction could be disposed of. After they had been washed with two cycles of 0.1% trifluoroacetic acid and 5% methanol in a 0.1% trifluoroacetic acid/H_2O mixture, the samples were eluted into a new Eppendorf tube with 4 μl elution buffer (50% acetonitrile in water). All steps used air pressure generated by the 10-μl pipette to drive the liquids through the resin bed. For MALDI-TOF mass spectrometry (MS) analysis the desalted recombinant human AS3MT samples were mixed with an equal volume of a saturated sinnapinic acid solution in 40% acetonitrile/60% H_2O containing 0.1% trifluoroacetic acid. One microliter was spotted on a polished steel target plate and allowed to air-dry prior to mass analysis. Reported masses are the average of three separate determinations. MS was performed using an Ultra flexII TOF/TOF mass spectrometer (Bruker Daltonics, Bremen, Germany) in linear mode with a 20-kV acceleration voltage.

Analysis of recombinant human AS3MT by western blot

The western-blot analysis of recombinant human AS3MT used mouse monoclonal anti-His-tag antibody (Tiangen Biotechnology). Samples from cultured cells, supernatant of cell lysate, and purified recombinant human AS3MT were dissolved in 2× SDS-PAGE sample buffer and boiled for 10 min. Proteins were resolved on 12% SDS-PAGE gel and electrophoretically transferred to a nitrocellulose membrane. The membrane was blocked with 5% nonfat milk in TBST buffer (10 mM Tris–HCl at pH 7.5, 150 mM NaCl, and 0.05% Tween 20) for 1 h at room temperature, and was

probed for 1 h at room temperature with mouse monoclonal anti-His-tag antibody (1:1,000) that was diluted with 5% nonfat milk. Following incubation with horseradish peroxidase conjugated goat–antimouse IgG antiserum (Santa Cruz Biotechnology, Santa Cruz, CA, USA) for 1 h at room temperature, recombinant human AS3MT protein was visualized with diaminobenzidine as a substrate.

UV–vis, CD, and fluorescence spectra

All spectra were recorded for the purified recombinant human AS3MT in 25 mM phosphate buffer (pH 7.0) at room temperature. UV–vis spectra were recorded using a PerkinElmer Lambda-35 spectrophotometer. Under the condition of the excitation wavelength of recombinant human AS3MT, 290 nm, the fluorescence spectra were recorded with a 48000 DSCF time-resolved fluorescence spectrometer (SLM, USA). CD (195–250 nm) spectra were recorded using a JASCO-J810 spectropolarimeter (JASCO, Japan) with 1-mm slit width and 10-mm light length. The scanning rate was set at 100 nm/min. The spectra were the average of three readings. The secondary structure parameters of recombinant human AS3MT were computed using Yang. Jwr software [44].

The spectra titrations of recombinant human AS3MT in the buffer were performed using a fixed protein concentration to which increments of the Se^{IV} stock solution (sodium selenite, Sigma) were added. Protein solutions employed were 4 μM in concentration and the concentration ratio of Se^{IV} to protein ranged from 0 to 1.2. Protein–Se^{IV} solutions were allowed to incubate for 5 min before the absorption spectra were recorded.

Activity assay

To optimize the reaction conditions, the reaction mixture (100 μl), containing iAs^{III} (0.5, 1.0, 3.0, 8.0, 15.0 μM), 1 mM *S*-adenosyl-L-methionine (SAM), and GSH or 1,4-dithiothreitol (DTT), cysteine, and 2-mercaptoethanol (2-ME) (0.5, 1.0, 3.0, 5.0, 7.0, 10.0 mM), and recombinant human AS3MT (1.0, 2.5, 5.0, 7.5, 10.0, 15.0, 20.0 μg) in 25 mM sodium phosphate buffer (pH 7.0), was incubated in a capped tube at 37 °C for 4 h. The concentration of SAM was determined in a previous study [16]. For the measurement of iAs^{III} methylation activity, the reaction mixture (100 μl), containing 1 μM iAs^{III}, 1 mM SAM, 7 mM GSH, and 10 μg recombinant human AS3MT in 25 mM sodium phosphate buffer (pH 7.0), was incubated at 37 °C for 4 h. To determine the effect of selenium on the activity of recombinant human AS3MT, the methylation of 1 μM iAs^{III} was examined by recombinant human AS3MT in the absence and presence of up to 1,000 μM Se^{IV}. Methylation rates were calculated as mole equivalents of methyl groups transferred from SAM to iAs^{III} (i.e., 1 nmol CH_3 per 1 nmol MMA^V or 2 nmol CH_3 per 1 nmol DMA^V). The reaction was quenched by boiling the samples for 5 min. Because trivalent arsenicals are known to bind to proteins [36, 45, 46], the methylation products of recombinant human AS3MT were treated with H_2O_2 (final concentration 10%) to oxidize all the arsenicals to the pentavalent form so that the arsenic metabolites can be released from the protein. Denatured proteins were removed by centrifugation and the supernatant of each sample was filtered though a 0.22-μm-pore membrane before measurement of arsenicals by high performance liquid chromatography inductively coupled plasma MS. Aliquots of reaction mixtures were chromatographed on an anion-exchange column (PRP X-100 250 mm × 4.6 mm inner diameter, 5 μm, Hamilton) using 15 mM $(NH_4)_2HPO_4$, adjusted to pH 6.0 with HCOOH, as

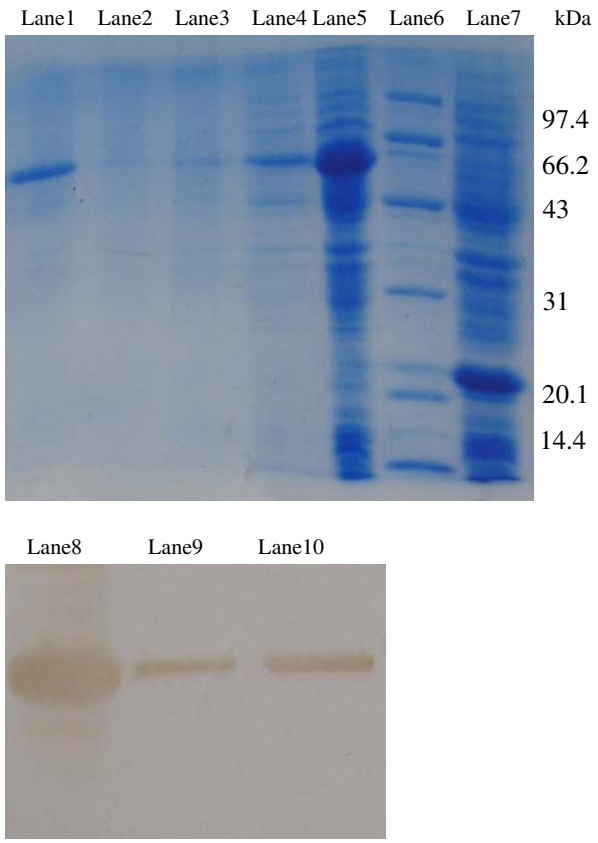

Fig. 3 Sodium dodecyl sulfate polyacrylamide gel electrophoresis (SDS-PAGE) and western-blot analysis of *Escherichia coli* expressed human AS3MT. **a** Coomassie blue stained 12% SDS-PAGE gel of fractions generated in the purification of recombinant human AS3MT. **b** Western-blot analysis performed using a monoclonal antibody against the 6× His-tag at 1:1,000 dilution. *Lane1* purified recombinant human AS3MT, *Lane2* wash fraction, *Lane3* flow-through fraction, *Lane4* soluble fraction, *Lane5* total proteins of induced cells, *Lane6* marker, *Lane7* total proteins of induced cells recombined with pET32a, *Lane8* recombinant human AS3MT in the induced cells, *Lane9* soluble fraction, *Lane10* purified recombinant human AS3MT

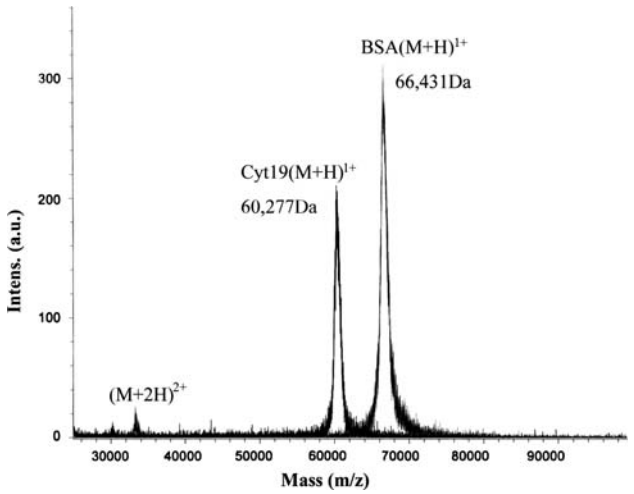

Fig. 4 Matrix-assisted laser desorption/ionization time of flight mass spectral analysis of purified recombinant human AS3MT. The results are the average of three determinations. Bovine serum albumin (*BSA*) was used as a standard protein

the mobile phase with a flow rate of 1.0 ml/min. Arsenicals of the separated species were detected using a Thermo X series II inductively coupled plasma mass spectrometer.

Results and discussion

Expression and purification of recombinant human AS3MT

The recombinant human AS3MT enzyme was expressed in *E. coli* with a Trx tag introduced at the N-terminus. SDS-PAGE and western-blot analyses of the recombinant human AS3MT in the cytoplasmic fraction of the IPTG-induced cells revealed the presence of distinct bands with molecular masses of about 60 kDa. A variety of bacteria growth temperatures and times were compared. The condition resulting in the best level of protein expression was 37 °C for 3 h. However, the recombinant human AS3MT protein was almost found in the inclusion bodies when the growth and the induction temperature were 37 °C, and recombinant protein purified from inclusion bodies was not successfully isolated in catalytically active form (data not presented). The culture conditions for the highest expressed activity were 5 h of incubation at 25 °C.

Culture conditions and the vector all contribute to modulating the proportion of soluble and insoluble forms of β-galactosidase, phospholipase A1, and so on [47–50]. Low-level expression may enhance the solubility and activity of difficult target proteins. Conditions that decrease the rate of protein synthesis, such as low induction temperatures, tend to raise the percentage of target protein

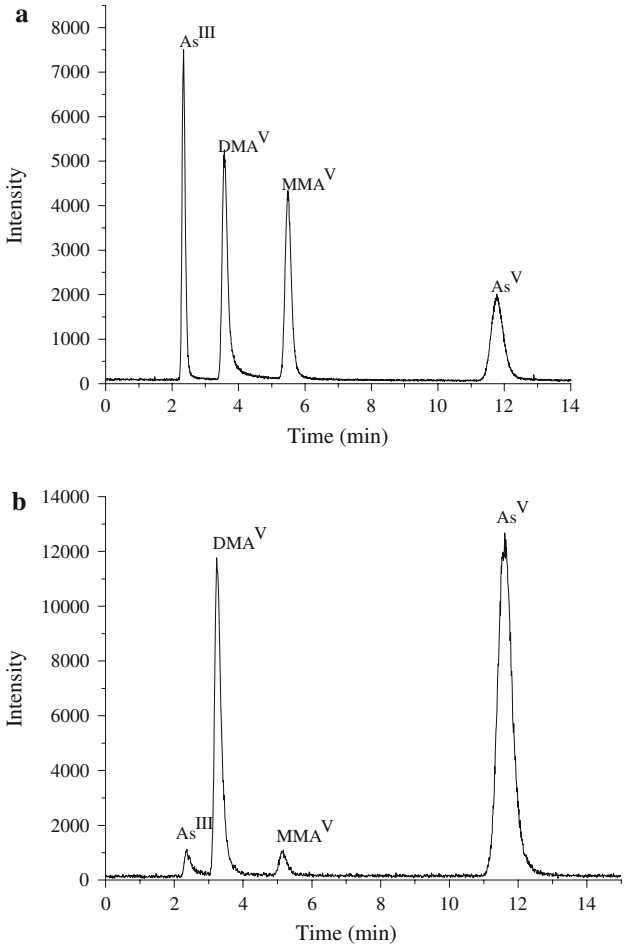

Fig. 5 Elution profiles of arsenicals on a PRP X-100 column by high performance liquid chromatography–inductively coupled plasma–mass spectrometry (HPLC–ICP-MS). A 20-µl portion of **a** authentic arsenicals such as inorganic As^{III} (iAs^{III}), dimethylarsinic acid (DMA^V), monomethylarsonic acid (MMA^V), and inorganic As^V and **b** arsenicals from an enzymatic assay mixture. The reaction mixture (100 µl), containing 10 µg recombinant human AS3MT, 1 mM *S*-adenosyl-L-methionine (SAM), 7 mM glutathione (GSH), and 1 µM iAs^{III} in 25 mM phosphate buffer (pH 7.0), was incubated at 37 °C for 4 h

found in soluble form [51]. Growth at 37 °C causes some proteins to accumulate as inclusion bodies, while incubation at 30 °C leads to a soluble, active protein [52]. In some cases, prolonged (e.g., overnight) induction at low temperatures (15–20 °C) may prove optimal for the yield of soluble protein. Growth and induction at 25 °C was optimal for the expression of a soluble and active form of recombinant human AS3MT.

The Trx·Tag™ fusion tag is a highly soluble polypeptide that can potentially enhance solubility of target proteins. Many proteins that are normally produced in an insoluble form in *E. coli* tend to become more soluble when fused with the N-terminal thioredoxin (Trx·Tag)

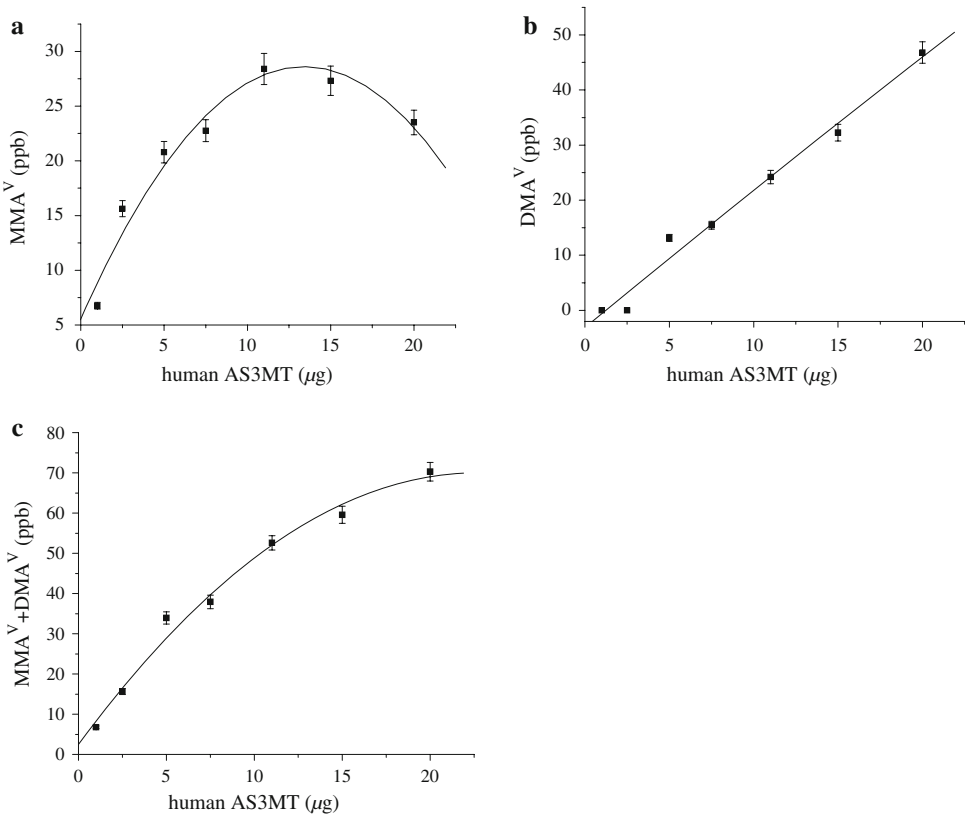

Fig. 6 Effect of concentrations of recombinant human AS3MT on methylation yields. Proportions of **a** MMA^V, **b** DMA^V, and **c** MMA^V plus DMA^V. The reaction mixture (100 µl), containing recombinant human AS3MT (1.0, 2.5, 5.0, 7.5, 10.0, 15.0, 20.0 µg), 1 mM SAM, 7 mM GSH, and 1 µM iAs^{III} in 25 mM phosphate buffer (pH 7.0), was incubated at 37 °C for 4 h. Each sample was applied to a PRP X-100 column and analyzed by HPLC–ICP-MS for speciation of arsenicals in the sample. The amount of each methylated arsenical was calculated by means of chromatography software. The data shown are means and standard deviations of three independent experiments

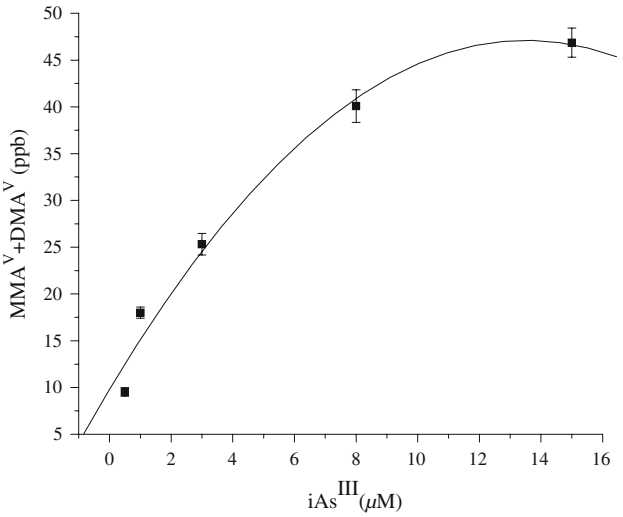

Fig. 7 Effect of concentrations of iAs^{III} on methylation yields. The reaction mixture (100 µl), containing 10 µg recombinant human AS3MT, 1 mM SAM, 7 mM GSH, and iAs^{III} (0.5, 1.0, 3.0, 8.0, 15.0 µM) in 25 mM phosphate buffer (pH 7.0), was incubated at 37 °C for 4 h. The data shown are means and standard deviations of three independent experiments

sequence [53]. When the pET-32a(+) vector designed for cytoplasmic expression is used, the Trx·Tag not only enhances the solubility of many target proteins, but also catalyzes the formation of disulfide bonds in the cytoplasm [54]. The combination of low expression temperature and coexpression of thioredoxin produced maximum levels of soluble, active, properly folded recombinant human AS3MT.

The supernatant fraction of cell lysate was loaded on a column packed with Ni-NTA agarose beads. Most of the soluble recombinant human AS3MT was bound to the column and minimally eluted in the flow-through fraction. The nonspecific proteins were removed from the Ni-NTA column through a series of washes with binding buffer and wash buffer. The catalytically active recombinant human AS3MT was eluted with elution buffer. Figure 3 shows a representative SDS-PAGE gel and western blot (using a monoclonal antibody against the 6× His-tag) in which the supernatant and purified recombinant human AS3MT appear as single bands with an apparent molecular mass of 60 kDa. The mass of recombinant human AS3MT was determined to be 60,277 ± 44 Da. The human AS3MT cDNA had a 1,125-bp open reading frame that encoded a 375 amino acid protein [55]. The human AS3MT cDNA sequence as well as that of the encoded protein are shown in Fig. 1. The recombinant human AS3MT in this study was a fusion protein which had a Trx·Tag, an S·Tag, and two His·Tags. Thus, the calculated molecular mass for the recombinant human AS3MT is 60,273 Da. The results of molecular mass measurements performed by MALDI-TOF-MS confirmed the identity of our purified protein as recombinant human AS3MT (Fig. 4).

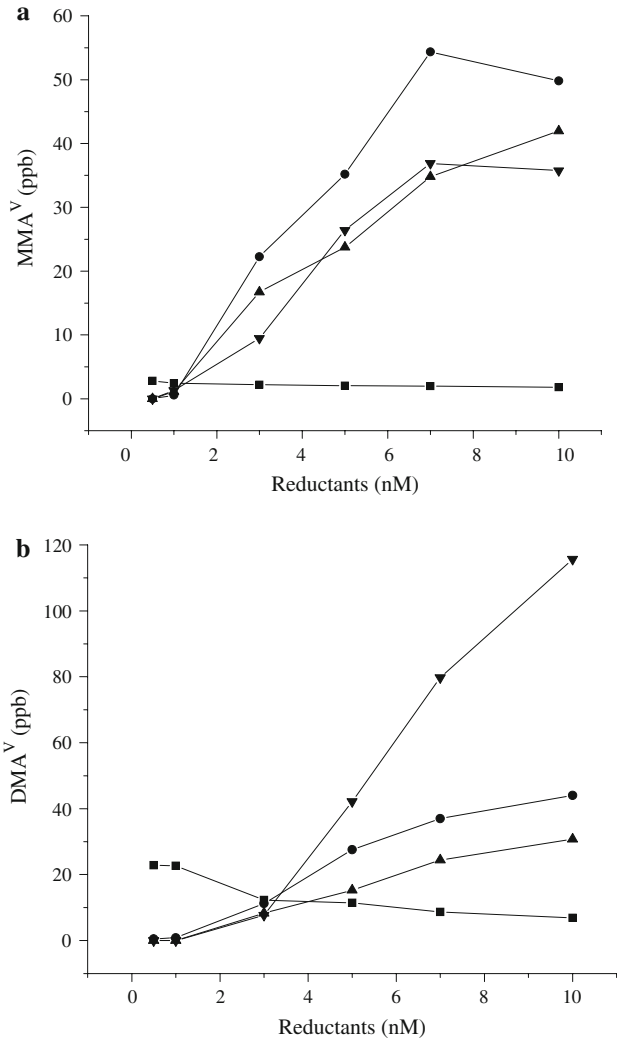

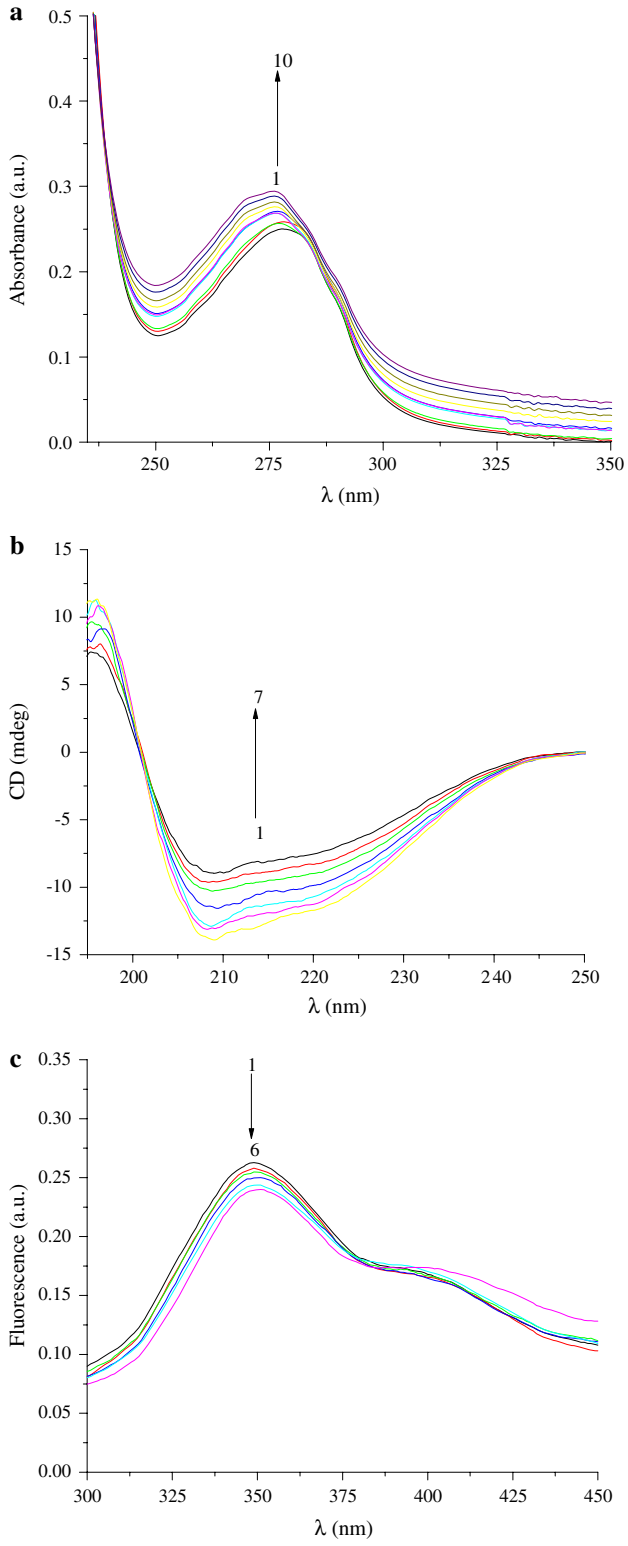

Fig. 8 Effect of concentrations of different reductants on methylation yields. Proportions of **a** MMA^V and **b** DMA^V. The reaction mixture (100 µl), containing 10 µg recombinant human AS3MT, 1 mM SAM, GSH (or 1,4-dithiothreitol, 2-mercaptoethanol, cysteine) (0.5, 1.0, 3.0, 5.0, 7.0, 10.0 mM), and 1 µM iAs^{III} in 25 mM phosphate buffer (pH 7.0), was incubated at 37 °C for 4 h. 1,4-Dithiothreitol (*squares*), GSH (*circles*), 2-mercaptoethanol (*upright triangles*), cysteine (*inverted triangles*)

Optimization of the methylation condition of iAs^{III} by recombinant human AS3MT

The recombinant human AS3MT could methylate arsenite to form MMA^V and DMA^V in vitro (Fig. 5). To optimize the reaction conditions, iAs^{III} methylation with various protein concentrations was investigated. Figure 6 shows the effect of the concentrations of recombinant human AS3MT on the production of MMA^V and DMA^V in the reaction mixture. The generation of DMA^V increased with the concentration of protein, whereas that of MMA^V initially increased with the concentration of recombinant human AS3MT, reaching a maximum value at 10 µg, and then decreased rapidly. The generation of total methylation products became saturated at 20 µg protein.

The recombinant human AS3MT methylated iAs^{III} at concentrations up to 1,000 µM. The generation of

◀ **Fig. 9** UV–vis, circular dichroism (*CD*), and fluorescence spectra of the recombinant human AS3MT in the absence and presence of increasing amounts of Se^{IV}. The concentration of recombinant human AS3MT was 4 μM. **a** Absorption spectra of recombinant human AS3MT in 25 mM phosphate buffer (pH 7.0) at room temperature in the absence and presence of Se^{IV}. The Se^{IV} to recombinant human AS3MT concentration ratios were 0, 0.1, 0.2, 0.4, 0.6, 0.7, 0.8, 0.9, 1.0, and 1.2, respectively. The *arrow* indicates the change in absorbance upon increasing Se^{IV} concentration. **b** CD spectra of recombinant human AS3MT in 25 mM phosphate buffer (pH 7.0) in the absence and presence of Se^{IV}. The Se^{IV} to recombinant human AS3MT concentration ratios were 0, 0.1, 0.3, 0.6, 0.9, 1.1, and 1.2, respectively. The *arrow* indicate the change in CD signal upon increasing Se^{IV} concentration. **c** Emission spectra of recombinant human AS3MT in 25 mM phosphate buffer (pH 7.0) in the absence and presence of Se^{IV}. The Se^{IV} to recombinant human AS3MT concentration ratios were 0, 0.1, 0.2, 0.4, 0.5, and 0.8, respectively. The *arrow* indicates the change in fluorescence intensity upon increasing Se^{IV} concentration. λ(excitation) and λ(emission) were 290 and 350 nm, respectively

methylation products increased with the concentration of iAs^{III} from 0 to 15 μM (Fig. 7). Purified recombinant human AS3MT enzyme followed apparent Michaelis–Menten kinetics with apparent K_m and V_{max} of 3.16 μM and 19.05 nmol/(mg h). The V_{max} of the recombinant human AS3MT was found to be higher than in an earlier study where the average methylation rate of recombinant rat AS3MT was 285 pmol CH_3 per milligram of protein per hour [28]. The reasons for the variation may be differences in sources of AS3MT and conditions used in the enzymatic assay, e.g., reductant and pH. At higher concentrations, the methylation activity of recombinant human AS3MT was inhibited. It is reported that higher concentrations of iAs^{III} may be toxic to recombinant protein [56]. The second methylation, from MMA^V to DMA^V, was probably inhibited by iAs^{III} [57].

The methylation reaction is inherently a redox process. It is generally accepted that inorganic arsenicals are metabolized by AS3MT through repetitive reduction and oxidative methylation to form pentavalent methylated arsenicals [10–16]. In the structure model of mouse AS3MT raised by Fomenko et al. [41], active-site cysteine was surface-exposed and protein topology supported the formation of an intramolecular disulfide during the catalytic cycle. This could imply that the methylation reaction is a redox-driven process with cysteine thiols getting oxidized. Oxidation of monothiols and dithiols has been linked to the reduction of As^V in organic arsenicals [58]. Thus, reductants play an important role in the methylation reaction. We performed extensive investigations of the effect of reductants on the function of recombinant human AS3MT (Fig. 8). The capacity of four reductants containing thiol, DTT, GSH, cysteine, and 2-ME, to support recombinant human AS3MT catalyzed formation of methylated arsenicals from arsenite was determined in reaction mixtures containing 10 μg recombinant human AS3MT, 1 mM AdoMet, a reductant, and 2 μM sodium arsenite in 25 mM sodium phosphate buffer (pH 7.0). In the absence of each reductant, no methylated metabolites were obtained. These reductants were about equipotent in supporting the conversion of arsenite to DMA^V, except DTT. Reductants (GSH, cysteine, and 2-ME) increased the methylation rates in concentration-dependent manners. MMA^V was the main methylated metabolite using cysteine as a reductant. The rate of formation of methylated metabolites decreased with increase of DTT concentrations. The mechanism for the methylation of iAs^{III} in the presence of DTT, a potent reductant, should be determined further.

Effects of the selenium compound on the structure and function of recombinant human AS3MT

The effect of selenium on the structure of recombinant human AS3MT was determined by UV–vis, CD, and fluorescence spectroscopy.

Figure 9a displays a well-behaved titration of recombinant human AS3MT with Se^{IV}. The intrinsic UV–vis absorption peak of recombinant human AS3MT at 278 nm is mainly caused by tryptophan and tyrosine in the recombinant human AS3MT. The titration of Se^{IV} induced large spectral perturbations in the specific absorption peak. The UV–vis spectra showed clearly that addition of Se^{IV} yielded hyperchromism and a slight blueshift. The hyperchromism and blueshift reached 17.77% and 2 nm, respectively. These spectral characteristics contributed to the change of the microenvironment of aromatic chromophores owing to the interaction between the recombinant human AS3MT and selenium.

Figure 9b shows the CD spectra for the recombinant human AS3MT in the absence and presence of increasing concentrations of Se^{IV} in the far-UV spectral region (190–250 nm). The CD spectra of recombinant human AS3MT showed a positive peak at 195 nm and two negative peaks at 208 and 222 nm, respectively. The recombinant human AS3MT was thus deduced to have a secondary structure of 29.0% α-helix, 23.9% β-pleated sheet, 17.9% β-turn, and 29.2% random coil. Protein secondary structure can be probed by CD spectroscopy in the far-UV [59, 60]. At these wavelengths the chromophore is the peptide bond, and the signal arises when it is located in a regular, folded environment. The α-helix, β-pleated sheet, and random coil structures each give rise to a characteristic shape and magnitude of the CD spectrum [60]. CD can also be used to follow changes in secondary structure with changes in solvent composition and changes in biomolecular interactions [61]. When Se^{IV} was added, the intensities of the positive peak and the two negative peaks decreased gradually, up to 35.54% (positive peak at 195 nm), 35.54% (negative peak at 208 nm), and 35.94% (negative peak at

222 nm). The content of the α-helix did not change, but that of the β-pleated sheet increased remarkably in the secondary conformation of recombinant human AS3MT.

The fluorescence spectra of recombinant human AS3MT in the absence and presence of increasing amounts of Se^{IV} are given in Fig. 9c. Under the excitation wavelength of 290 nm, recombinant human AS3MT had maximal fluorescence at a wavelength of about 350 nm. The result showed that tryptophan residues were exposed to water, not buried in the internal environment of the recombinant human AS3MT. Proteins contain three aromatic amino acid residues (tryptophan, tyrosine, phenylalanine) which may contribute to their intrinsic fluorescence [62]. Tryptophan has the strongest fluorescence and highest quantum yield among the three aromatic amino acids [62]. The wavelength of the emitted light is a good indication of the environment of the fluorophore [63]. The fluorescence can be used to monitor structural changes in the protein [64]. Tryptophan fluorescence appears to be uniquely sensitive to collisional quenching, either by externally added quenchers or by nearby protonated acidic groups in the protein [62, 64, 65]. The recombinant human AS3MT has three tryptophan residues (Trp73, Trp203, and Trp213), each of which is located on the side of a protonated acidic group (Asp76 or Glu205 and Glu215) and a cysteine residue (Cys72, Cys206, and Cys226). The fluorescence of recombinant human AS3MT was quenched gradually with increasing concentrations of Se^{IV}. We hypothesized that Se^{IV} might modify the structure of recombinant human AS3MT owing to its combining with the sulfhydryl group of the cysteine residue, and then tryptophan fluorescence might be quenched by neighboring protonated acidic groups.

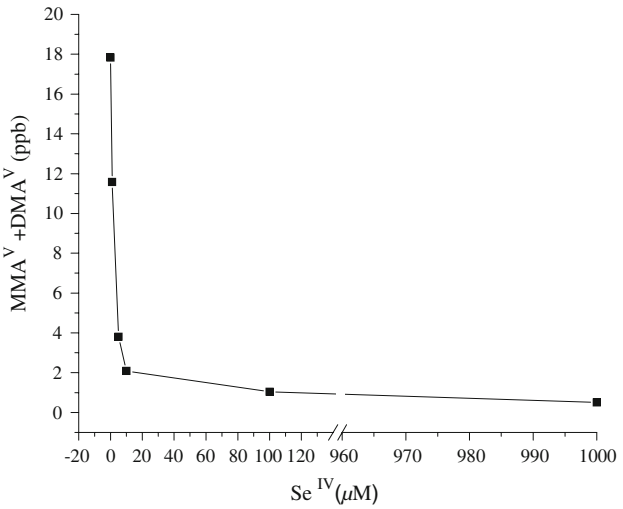

Fig. 10 Modulation of AS3MT activity of the recombinant human AS3MT by Se^{IV}. The reaction mixture (100 µl), containing 10 µg recombinant human AS3MT, 1 mM SAM, 7 mM GSH, and 1 µM iAs^{III} in 25 mM phosphate buffer (pH 7.0), was incubated at 37 °C for 4 h

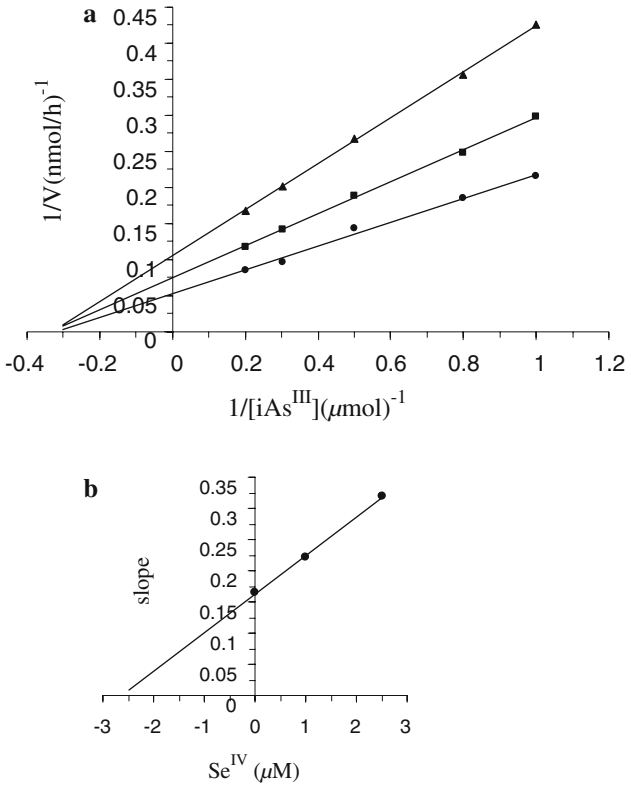

Fig. 11 Double-reciprocal plots for the inhibitor of the recombinant human AS3MT by Se^{IV}. **a** Double-reciprocal plots. **b** Replot of slopes of the corresponding double-reciprocal plots versus concentration of inhibitor. The reaction mixtures (100 µl), containing 10 µg recombinant human AS3MT, 1 mM SAM, 7 mM GSH, and 1, 1.25, 2, 3.3, and 5 µM iAs^{III} in 25 mM phosphate buffer (pH 7.0), were incubated at 37 °C for 4 h. Plots for 0 µM Se^{IV} (*circles*), 1.0 µM Se^{IV} (*squares*), and 2.5 µM Se^{IV} (*triangles*)

Se^{IV} inhibited the enzymatic methylation of arsenite in a concentration-dependent manner (Fig. 10). The IC_{50} value for Se^{IV} was 2.38 µM. Kinetic analysis characterized the inhibition of recombinant human AS3MT by Se^{IV} over a range of iAs^{III} concentrations from 1 to 5 µM. Double-reciprocal ($1/V$ vs. $1/[iAs^{III}]$) plots showed Se^{IV} to be a noncompetitive inhibitor of the methylation of iAs^{III} by recombinant human AS3MT (Fig. 11a). The K_i value of 2.61 µM was obtained from the replot of the slopes of the corresponding double-reciprocal plots versus concentration of Se^{IV} (Fig. 11b).

The mechanisms by which Se^{IV} inhibits AS3MT activity are unclear. The inhibition of enzyme activity by selenium compounds was attributed to their affinity for thiols at the active site of the enzyme [40]. Fomenko et al. [41] confirmed that Cys157 and Cys207 were the active sites of the recombinant mouse AS3MT using high-throughput identification of catalytically redox active cysteine residues and site-directed mutagenesis. The active sites of recombinant

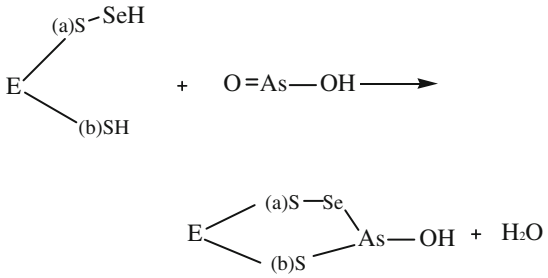

E: recombinant human AS3MT

(a) S: cysteine in the structural residues

(b) S: cysteine in the active center

Scheme 1 The possible mechanism of the formation of the inhibitory complex

human AS3MT were deduced to be Cys156 and Cys206 by protein sequence alignment analysis. Walton et al. [28] reported that Se^{IV} could effectively inhibit the methylation of recombinant rat AS3MT in a competitive manner. Our experiments gave different findings. Se^{IV} was a noncompetitive inhibitor of the methylation of iAs^{III} by the recombinant human AS3MT. Given the high affinity of Se^{IV} for thiols [66], we hypothesized that Se^{IV} probably interacts with one or several cysteines in the structural residues of recombinant human AS3MT rather than the cysteines of the active site (Cys156 and Cys206). These cysteine residues probably play an important role in supporting the conformation of recombinant human AS3MT. When Se^{IV} was combined with cysteine(s) in the structural residues, the conformation of recombinant human AS3MT changed and the activity decreased. Levander et al. [67] put forward a possible role of this arsenic/selenium antagonism in metabolism. It was suggested that a peculiar grouping might be a selenopersulfide in close proximity to a thiol. Perhaps an inhibitory complex would be formed as shown in Scheme 1 [25]. Considering the quenching of tryptophan fluorescence, Cys72 and/or Cys226 may be primary targets for Se^{IV}. The effects of selenium structure and function of AS3MT were both concentration-dependent. These results might be a sound explanation for the relationship between the structure and function of recombinant human AS3MT.

Conclusions

Under the optimal conditions, soluble and active recombinant human AS3MT was expressed in *E. coli* with a Trx tag introduced at the N-terminus. UV–vis, CD, and fluorescence spectra were firstly used to study the interactions between recombinant human AS3MT and Se^{IV}. Further studies showed that Se^{IV} was a noncompetitive inhibitor of the methylation of iAs^{III} by the recombinant human AS3MT. Given the affinity of Se^{IV} for thiols, Se^{IV} could be combined with one or several cysteines in the structural residues of human AS3MT. In a future study, cysteines in the structural residues will be mutated by the use of site-directed mutagenesis. Effects of selenium on the structures and function of those human AS3MT mutants will contribute to locating the site(s) where selenium binds to the cysteine(s) of human AS3MT.

Acknowledgments This work was supported by the National Natural Science Foundation of China (20535020, 20671051, 20721002, and 90813020) and the National Basic Research Program of China (2007CB925102).

References

1. Chowdhury TR, Basu GK, Mandal BK, Raymahashay BC, Guha S, Bhowmik A (1999) Nature 401:545–547
2. Stokstad E (2002) Science 298:1535–1537
3. Islam FS, Gault AG, Boothman C, Polya DA, Charnock JM, Chatterjee D, Lloyd JR (2004) Nature 430:68–71
4. Sun GF (2004) Toxicol Appl Pharmacol 198:268–271
5. Tchounwou PB, Centeno JA, Patlolla AK (2004) Mol Cell Biochem 255:47–55
6. Chen CJ, Chen CW, Wu MM, Kuo TL (1992) Br J Cancer 66:888–892
7. Bates MN, Smith AH, Hopenhaynrich C (1992) Am J Epidemiol 135:462–476
8. Smith AH, Hopenhaynrich C, Bates MN, Goeden HM, Hertzpicciotto I, Duggan HM, Wood R, Kosnett MJ, Smith MT (1992) Environ Health Perspect 97:259–267
9. Buchet JP, Lauwerys R, Roels H (1981) Int Arch Occup Environ Health 48:71–79
10. Smith TJ, Crecelius EA, Reading JC (1977) Environ Health Perspect 19:89–93
11. Crecelius EA (1977) Environ Health Perspect 19:147–150
12. Cullen WR, McBride BC, Reglinski J (1984) J Inorg Biochem 21:45–60
13. Cullen WR, McBride BC, Reglinski J (1984) J Inorg Biochem 21:179–194
14. Lin S, Shi Q, Nix FB, Styblo M, Beck MA, Herbin-Davist KM, Hall LL, Simeonsson JB, Thomas DJ (2002) J Biol Chem 277:10795–10893
15. Thomas DJ, Waters SB, Styblo M (2004) Toxicol Appl Pharmacol 198:319–326
16. Drobna Z, Waters SB, Deves V, Harmon AW, Thomas DJ, Styblo M (2005) Toxicol Appl Pharmacol 207:147–159
17. Hayakawa T, Kobayashi Y, Cui X, Hirano S (2005) Arch Toxicol 79:183–191
18. Styblo M, Thomas DJ (2001) Toxicol Appl Pharmacol 172:52–61
19. Hasegawa T, Okuno T, Nakamuro K, Sayato Y (1996) Arch Toxicol 71:39–44
20. Tarze A, Dauplais M, Grigoras I, Lazard M, Ha-Duong NT, Barbier F, Blanquet S, Plateau P (2007) J Biol Chem 282:8759–8767
21. Ganther HE (1971) Biochemistry 10:4089–4098
22. Francesconi KA, Pannier F (2004) Clin Chem 50:2240–2253
23. Mozier NM, McConnell KP, Hoffman JL (1988) J Biol Chem 263:4527–4531
24. Ranjard L, Prigent-Combaret C, Nazaret S, Cournoyer B (2002) J Bacteriol 184:3146–3149

25. Levander OA (1977) Environ Health Perspect 19:159–164
26. Babich H, Martin-Alguacil N, Borenfreund E (1989) Toxicol Lett 45:157–164
27. Biswas S, Talukder G, Sharma A (1999) Mutat Res 441:155–160
28. Walton FS, Waters SB, Jolley SL, LeCluyse EL, Thomas DJ, Styblo M (2003) Chem Res Toxicol 16:261–265
29. Kenyon EM, Hughes MF, Levander OA (1997) J Toxicol Environ Health 51:279–299
30. Ueda H, Kuroda K, Endo G (1997) Anticancer Res 17:1939–1944
31. Gregus Z, Gyurasics A, Koszorus L (1998) Environ Toxicol Pharmacol 5:89–99
32. Miyazaki K, Watanabe C, Mori K, Yoshida K, Ohtsuka R (2005) Toxicology 208:357–365
33. Hsueh YM, Ko YF, Huang YK, Chen HW, Chiou HY, Huang YL, Yang MH, Chen CJ (2003) Toxicol Lett 137:49–63
34. Christian WJ, Hopenhayn C, Centeno JA, Todorov T (2006) Environ Res 100:115–122
35. Beckman L, Nordenson I (1986) Hum Hered 36:397–401
36. Styblo M, Delnomdedieu M, Thomas DJ (1996) Chem Biol Interact 99:147–161
37. Manley SA, George GN, Pickering IJ, Glass RS, Prenner EJ, Yamdagni R, Wu Q, Gailer J (2006) Chem Res Toxicol 19:601–607
38. Gailer J, George GN, Pickering IJ, Prince RC, Younis HS, Winzerling JJ (2002) Chem Res Toxicol 15:1466–1471
39. Gailer J, George GN, Pickering IJ, Prince RC, Ringwald SC, Pemberton JE, Glass RS, Younis HS, DeYoung DW, Aposhian HV (2000) J Am Chem Soc 122:4637–4639
40. Zakharyan RA, Tsaprailis G, Chowdhury UK, Hernandez A, Aposhian HV (2005) Chem Res Toxicol 18:1287–1295
41. Fomenko DE, Xing W, Adair BM, Thomas DJ, Gladyshev VN (2007) Science 315:387–389
42. Kuroki T, Matsushima T (1987) Mutagenesis 2:33–37
43. Sanger F, Nicklen S, Coulson AR (1977) Proc Natl Acad Sci USA 74:5463–5467
44. Yang JT, Chuen-Shang CW, Martinez HM (1986) Method Enzymol 130:208–257
45. Styblo M, Thomas DJ (1997) Toxicol Appl Pharmacol 147:1–8
46. Naranmandura H, Suzuki N, Suzuki KT (2006) Chem Res Toxicol 19:1010–1018
47. Blackwell JR, Horgan R (1991) FEBS Lett 295:10–12
48. Moore JT, Uppal A, Maley F, Maley GF (1993) Protein Expres Purif 4:160–163
49. Strandberg L, Enfors SO (1991) Appl Environ Microbiol 57:1669–1674
50. Song JK, Kim MK, Rhee JS (1999) J Biotechnol 72:103–114
51. Schein CH, Noteborn MHM (1988) Nat Biotechnol 6:291–294
52. Schein CH (1989) Nat Biotechnol 7:1141–1149
53. LaVallie ER, DiBlasio EA, Kovacic S, Grant KL, Schendel PF, McCoy JM (1993) Nat Biotechnol 11:187–193
54. Stewart EJ, Åslund F, Beckwith J (1998) EMBO J 17:5543–5550
55. Wood TC, Salavagionne OE, Mukherjee B, Wang L, Klumpp AF, Thomae BA, Eckloff BW, Schaid DJ, Wieben ED, Weinshilboum RM (2006) J Biol Chem 281:7364–7373
56. Styblo M, Del Razo LM, Vega L, Germolec DR, LeCluyse EL, Hamilton GA, Reed W, Wang C, Cullen WR, Thomas DJ (2000) Arch Toxicol 74:289–299
57. Kobayashi Y, Hayakawa T, Hirano S (2007) Environ Toxicol Pharmacol 23:115–120
58. Buchet JP, Lauwerys R (1988) Biochem Pharmacol 37:3149–3153
59. Bode KA, Applequist J (1998) J Am Chem Soc 120:10938–10946
60. Hennessey JP Jr, Johnson WC Jr (1981) Biochemistry 20:1085–1094
61. Manavalan P, Johnson WC Jr (1985) Proc Int Symp Biomol Struct Interact Suppl J Biosci 8:141–149
62. Chen Y, Barkley MD (1998) Biochemistry 37:9976–9982
63. Vivian JT, Callis PR (2001) Biophys J 80:2093–2109
64. Gensch T, Hendriks J, Hellingwerf K (2004) Photochem Photobiol Sci 3:531–536
65. Weljie AM, Vogel HJ (2000) Protein Eng 13:59–66
66. Ganther HE (1999) Carcinogenesis 20:1657–1666
67. Levander OA, Morris VC, Higgs DJ (1973) Biochemistry 12:4591–4595